Development 136, 2059-2067 (2009) doi:10.1242/dev.035444

Dynamic, auxin-responsive plasma membrane-to-nucleus movement of *Arabidopsis* BRX

Emanuele Scacchi[1,*], Karen S. Osmont[1,*], Julien Beuchat[1], Paula Salinas[1], Marisa Navarrete-Gómez[2], Marina Trigueros[2], Cristina Ferrándiz[2] and Christian S. Hardtke[1,†]

In *Arabidopsis*, interplay between nuclear auxin perception and trans-cellular polar auxin transport determines the transcriptional auxin response. In *brevis radix* (*brx*) mutants, this response is impaired, probably indirectly because of disturbed crosstalk between the auxin and brassinosteroid pathways. Here we provide evidence that BRX protein is plasma membrane-associated, but translocates to the nucleus upon auxin treatment to modulate cellular growth, possibly in conjunction with NGATHA class B3 domain-type transcription factors. Application of the polar auxin transport inhibitor naphthalene phthalamic acid (NPA) resulted in increased BRX abundance at the plasma membrane. Thus, nuclear translocation of BRX could depend on cellular auxin concentration or on auxin flux. Supporting this idea, NPA treatment of wild-type roots phenocopied the *brx* root meristem phenotype. Moreover, BRX is constitutively turned over by the proteasome pathway in the nucleus. However, a stabilized C-terminal BRX fragment significantly rescued the *brx* root growth phenotype and triggered a hypocotyl gain-of-function phenotype, similar to strong overexpressors of full length BRX. Therefore, although BRX activity is required in the nucleus, excess activity interferes with normal development. Finally, similar to the PIN-FORMED 1 (PIN1) auxin efflux carrier, BRX is polarly localized in vascular cells and subject to endocytic recycling. Expression of *BRX* under control of the *PIN1* promoter fully rescued the *brx* short root phenotype, suggesting that the two genes act in the same tissues. Collectively, our results suggest that BRX might provide a contextual readout to synchronize cellular growth with the auxin concentration gradient across the root tip.

KEY WORDS: Plants, Hormones, Auxin, *Arabidopsis*, BRX, PIN1, Root meristem, Endocytosis

INTRODUCTION

The establishment of cell polarity in a coordinated tissue context is a common phenomenon in multicellular eukaryotes. In plants, such polarity often requires directional transport of the phytohormone auxin, known as polar auxin transport (PAT) (Men et al., 2008; Reinhardt et al., 2000; Sauer et al., 2006). PAT is important throughout plant development, for instance in the formation and placement of lateral organs. Proper local auxin activity is conveyed by the interplay between nuclear auxin signaling and trans-cellular PAT, and molecular mechanisms for both processes have recently been well defined (Benjamins and Scheres, 2008; Leyser, 2005). PAT requires the activity of integral plasma membrane auxin efflux carriers, the PIN-FORMED (PIN) proteins (Wisniewska et al., 2006), whose polar cellular localization is crucial for the establishment of complex auxin flux patterns, needed for embryo axis formation and root growth, for example (Blilou et al., 2005; Friml et al., 2003; Grieneisen et al., 2007; Sabatini et al., 1999). Several PIN family genes are feedback-controlled by transcriptional regulators that convey cellular auxin concentration into gene expression responses (Sauer et al., 2006; Vieten et al., 2005). This is mediated by auxin receptors such as TRANSPORT INHIBITOR RESPONSE 1 (TIR1), the F-box component of the E3 ubiquitin ligase complex that targets transcriptional corepressors of the auxin/indole-3-acetic acid (AUX/IAA) family for proteasome-mediated degradation (Dharmasiri et al., 2005a; Dharmasiri et al., 2005b; Kepinski and Leyser, 2005). Affinity of AUX/IAA proteins for TIR1-type auxin receptors is enhanced by the latter binding to auxin. Thus, auxin promotes AUX/IAA degradation. Since AUX/IAA inhibits the activation potential of auxin response factors (ARFs), this releases ARFs to activate transcriptional targets of auxin signaling (Benjamins and Scheres, 2008; Tiwari et al., 2004).

Despite this impressive progress, it appears that auxin signaling may be even more complex and may involve unidentified components (Badescu and Napier, 2006; Benjamins and Scheres, 2008; Strader et al., 2008). For instance, rapid effects of auxin on cellular growth are difficult to account for with the canonical auxin signaling pathway described above (Badescu and Napier, 2006), and indeed auxin-responsive pathways that do not involve the TIR1-type auxin receptors appear to exist (Strader et al., 2008).

The *Arabidopsis* gene *BREVIS RADIX* (*BRX*) is a more recently identified rate-limiting component for auxin-responsive gene expression. *brx* mutants display impaired root growth due to decreased cell proliferation in the root meristem and vasculature and generally reduced cell elongation (Mouchel et al., 2004; Sibout et al., 2008). Global gene expression analyses have indicated that auxin-responsive gene expression is impaired in *brx* mutants, affecting expression of the synthetic auxin response reporter gene, *DR5::GUS* (Mouchel et al., 2006). This is likely to be the result of effects on brassinosteroid biosynthesis, as the *brx* phenotype and impaired *DR5::GUS* expression can be significantly rescued by exogenous application of this class of phytohormones (Mouchel et al., 2006). These findings are part of accumulating evidence for a rate-limiting role of the brassinosteroid pathway in the auxin response (Hardtke, 2007; Kuppusamy et al., 2008; Nemhauser et al., 2004; Vert et al., 2008). Interestingly, expression of *BRX* is itself strongly induced by auxin (Mouchel et al., 2006). Consistently, *BRX* expression is no longer auxin-responsive in *brx* mutants, suggesting that auto-regulatory feedback exists. In this study, we investigated

[1]Department of Plant Molecular Biology, University of Lausanne, Biophore Building, CH-1015 Lausanne, Switzerland. [2]Instituto de Biología Molecular y Celular de Plantas, UPV-CSIC, 46022 Valencia, Spain.

*These authors contributed equally to this work
†Author for correspondence (e-mail: christian.hardtke@unil.ch)

Accepted 10 April 2009

auxin control of *BRX* in more detail, revealing that BRX might be part of a novel, context-specific auxin signaling pathway that could serve to modulate cellular growth along the auxin concentration gradient of the root tip.

MATERIALS AND METHODS

Plant materials

Seeds were stratified 2-4 days at 4°C before transfer into constant light of 120 μE intensity on 0.5 × Murashige and Skoog (MS) media. Transgenic plants were generated according to standard procedures as previously described (Mouchel et al., 2004). The brx^S, brx^C, brx^C *brxl1*, *pBRX::BRX:GFP*, *p35S::BRX:GFP* and *pRCP1::BRX:GFP* lines have been described (Mouchel et al., 2004; Mouchel et al., 2006). brx^S: introgression of the natural Uk-1 *brx* loss-of-function allele into the Sav-0 background; brx^C: introgression of the natural Uk-1 *brx* loss-of-function allele into the Col-0 background; the *p35S::BRX:GFP* (with the N- and C-terminal fragment fusions with GFP) were created in the pMDC83 vector (Curtis and Grossniklaus, 2003). Hormone and inhibitor treatments were carried out in liquid media or on plates. All reagents were stored as frozen, small aliquots of stock solution and not reused after thawing.

Molecular biology and biochemistry

Molecular biology and biochemistry procedures were carried out according to standard protocols. BRX-GFP and GFP were detected using a monoclonal anti-GFP antibody (JL-8; Clontech, USA), whereas RNA polymerase I subunit TFIIS and H^+-ATPase were detected using antibodies against the endogenous protein (Agrisera, Sweden). GUS stainings of *pBRX::GUS* and *pBRXL1::GUS* plants were performed as described (Mouchel et al., 2006).

Root gravitropism assays

Seeds were stratified and then transferred into constant light for 24 hours to promote germination before being grown vertically in the dark for 2 days. To provoke gravitropic response, plates were then rotated 90° and grown for another 24 hours. Plates were scanned on a flat bed scanner immediately before and after, and reorientation of root growth was scored with ImageJ software (version 1.36b).

Microscopy

For confocal microscopy, roots of 3- to 4-day-old seedlings grown on solid media were placed in liquid media including any treatments before analysis using a Leica SP2 AOBS confocal laser scanning microscope (CLSM). All images were taken with an offset of less than 5%. Intensity correlation analysis and Manders' overlap coefficient calculation were performed as described (Li et al., 2004; Manders et al., 1993) using an ImageJ plugin (http://www.macbiophotonics.ca/imagej/colour_analysis.htm). For analysis of embryo phenotypes, ovules were collected and fixed in chloral hydrate:glycerol:H_2O (8:3:1) solution. Microscopy was then performed using a Leica DM5000B compound microscope.

Microsomal fractionation

To isolate membranes, 6-day-old seedlings were ground in extraction buffer (400 mM glucose, 100 mM Tris pH 7.5, 1 mM EDTA, 1 mM PMSF) and centrifuged at 1000 ***g*** for 10 minutes to eliminate debris. The supernatant was filtered through two layers of Miracloth and again centrifuged, at 8000 ***g*** for 15 minutes. The supernatant was then centrifuged at 150,000 ***g*** for 1 hour to yield a pellet containing membrane fractions and supernatant containing soluble protein (Bassham and Raikhel, 1998).

In planta bimolecular fluorescence complementation

Open reading frames of full length NGA1 and BRX, as well as BRX C- and N-terminal fragments, were cloned into vectors $pYFP^N43$ and $pYFP^C43$ (kindly provided by A. Ferrando, University of Valencia, Burjassot, Valencia, Spain). These different binary vectors were introduced into *Agrobacterium tumefaciens* strain C58C1 (pGV2260) and grown in Luria-Bertani medium to late exponential phase. Cells were harvested by centrifugation and resuspended (10 mM MES-KOH, pH 5.6, 10 mM $MgCl_2$, 150 μM acetosyringone) to an OD_{600} of 1. The cells were mixed with an equal volume of strain C58C1 (pCH32 35S:p19), which expresses the silencing suppressor p19 of tomato bushy stunt virus (Voinnet et al., 2003), so that the final density of *Agrobacterium* solution was 1. Bacteria were then incubated for 3 hours at room temperature before being injected into young, fully expanded leaves of 4-week-old tobacco plants. Leaves were examined after 3 to 4 days by confocal microscopy.

RESULTS

BRX is required for correct transcriptional auxin response

Previous physiological and gene expression analyses have suggested that auxin-responsive gene expression is impaired in *brx* null mutants (Mouchel et al., 2006). However, *brx* root growth was still responsive to exogenous application of the prototypical natural auxin, indole-3-acetic acid (IAA; Fig. 1A), suggesting that auxin perception by the canonical auxin signaling pathway is principally intact in the mutant. To better understand the manner in which loss of *BRX* function affects auxin-responsive gene expression, we took advantage of another *Arabidopsis* mutant, *elongated hypocotyl 5* (*hy5*), which has been shown to display constitutively elevated expression of auxin-responsive genes

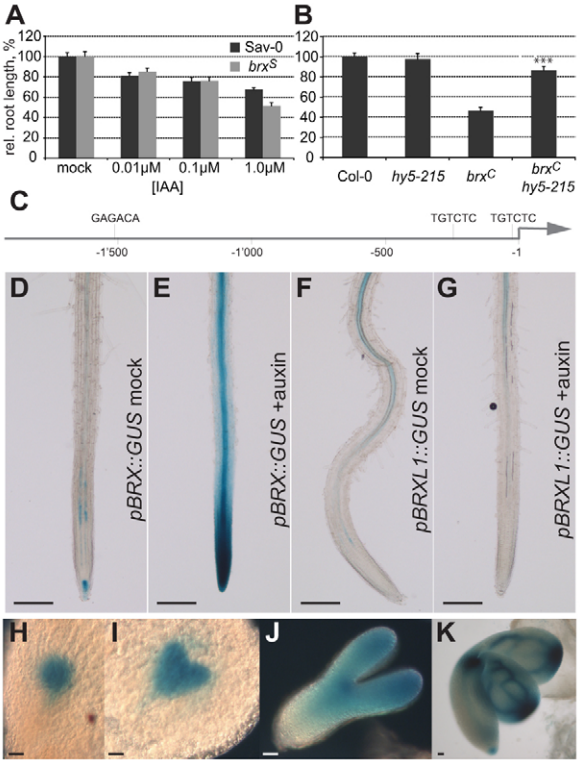

Fig. 1. Auxin-induced and embryonic expression of *BRX*. (**A**) Auxin [indole-3-acetic acid (IAA), the major natural auxin] inhibition of primary root growth of wild-type versus *brx* mutant seedlings measured at 7 days after germination (dag). (**B**) Primary root growth in *hy5* (*hy5-215* null allele), brx^C and the *hy5-215* brx^C double mutant measured at 9 dag. (**C**) Schematic overview of the *BRX* promoter region and the localization of ARF binding sites. (**D**,**E**) Transgenic plants expressing the *GUS* reporter gene under control of the *BRX* promoter (*pBRX::GUS*) stained for GUS activity after mock (D) or auxin (10 μM IAA for 1 hour, E) treatment. (**F**,**G**) Similar to D,E for the *BRXL1* promoter. (**H-K**) Expression of *pBRX::GUS* during embryogenesis, from globular (H) via early heart (I) and torpedo stage (J), up to mature embryos (K). Scale bars: 0.5 mm in D-G; 50 μm in H-K. Error bars represent standard error of the mean, ***P<0.001.

(Sibout et al., 2006). Strikingly, introduction of the *hy5* mutation into the *brx* background resulted in significant rescue of the *brx* root growth phenotype (Fig. 1B), suggesting that basic auxin-responsiveness of the transcriptional machinery is diminished in *brx* mutants.

Auxin-responsive and embryonic expression of *BRX*

In line with the auxin-responsiveness of *BRX* transcription, the *BRX* promoter contains several auxin-responsive elements, among them two prototypical ARF binding sites (Ulmasov et al., 1997) close to the transcription initiation site (Fig. 1C). Consistently, expression of the β-glucuronidase reporter gene (*GUS*) under control of the *BRX* promoter (*pBRX::GUS*) was auxin-inducible (Fig. 1D-E), whereas expression under the control of the promoter of the homologous gene *BRXL1*, which does not contain ARF binding sites, was not (Fig. 1F-G). This difference possibly contributes to the expression level difference and thus the lack of functional redundancy between the two genes, as *BRXL1* can replace *BRX* if expressed constitutively under control of the *35S* promoter (Briggs et al., 2006). Redundancy also appears limited because of overlapping but not identical expression patterns (Fig. 1D,F). For instance, whereas *BRXL1* expression was observed in the root vasculature, similar to *BRX*, this was largely restricted to mature tissue. By contrast, *BRX* was expressed throughout all root phloem vasculature as well as in the root tip, in a pattern that was remarkably similar to the expression pattern of *DR5::GUS* (Mouchel et al., 2006). Notably, auxin response is of pivotal importance during embryogenesis and it has been previously suggested that *BRX* activity might be required at this stage (Mouchel et al., 2006). Indeed, analysis of *pBRX::GUS* expression in embryos revealed that *BRX* is ubiquitously expressed at early stages and becomes restricted to the (incipient) vasculature in the mature embryo and at later stages of (adult) development (Fig. 1H-K) (Bauby et al., 2007).

brx mutants display embryo phenotypes reminiscent of auxin pathway mutants

In *Arabidopsis*, embryogenesis progresses through a series of stereotypical cell divisions that eventually lead to the formation of an apical-basal embryo axis. Several key players in auxin signaling and PAT, including PINs, are required for this process and respective mutants show embryonic phenotypes of variable penetrance and severity, depending on allele strengths and genetic redundancies (Blilou et al., 2005; Hamann et al., 2002; Hardtke and Berleth, 1998; Hardtke et al., 2004). Similarly, we found that a significant portion of *brx* embryos displayed defects in the stereotypical arrangement of cells in the basal layers that strongly resembled those of auxin signaling or transport mutants from as early as the dermatogen stage (Fig. 2A-H). Moreover, this portion significantly increased in *brx brxl1* double mutants (Fig. 2I), suggesting redundancy of the two homologs during embryogenesis. Therefore, our data suggest that *BRX* expression during embryogenesis is physiologically relevant and more important than previously recognized.

Auxin negatively regulates BRX protein abundance

A salient feature of AUX/IAA corepressors is that while their abundance is negatively regulated by auxin, their respective genes are themselves primary auxin-induced genes, establishing a negative-feedback loop (Benjamins and Scheres, 2008; Dharmasiri et al., 2005a; Gray et al., 2001; Kepinski and Leyser, 2005). To determine whether *BRX* is also controlled at multiple levels, we investigated the behavior of the BRX protein. This was primarily done by monitoring the functional BRX-GFP (green fluorescent protein) fusion protein expressed under control of the constitutive *35S* promoter (*p35S::BRX:GFP*), as BRX-GFP expressed from its endogenous promoter (*pBRX::BRX:GFP*) was not detectable in western blots. Investigation of BRX-GFP fusion protein behavior in response to auxin treatment revealed that, strikingly, auxin negatively regulated BRX-GFP abundance. The degree of this response was variable in replicate experiments, but occasionally led to nearly total disappearance of the protein (Fig. 3A). Moreover, treatment with the proteasome inhibitor MG132 could interfere with this degradation and led to accumulation of BRX-GFP (Fig. 3B). Since neither control protein nor GFP alone displayed these characteristics, we concluded that BRX must be a target for auxin-induced, proteasome-mediated degradation.

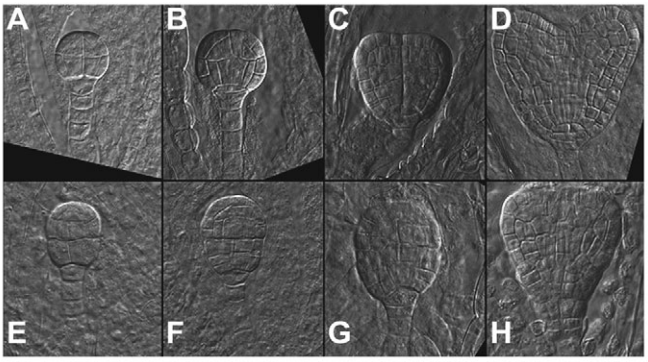

I

	Col-0	*brx*^{C}	*brx*^{C} *brxl1*	*p35S::BRX* in Uk-1	Uk-1
% aberrant embryos	1.17% (n=256)	5.38% (n=130)	11.31% (n=168)	1.32% (n=227)	6.03% (n=232)
Chi-square test:		p<0.001	p<0.001		p<0.005

Fig. 2. Embryo phenotypes in *brx* loss-of-function mutants. (**A-D**) Microscopic images (Nomarski optics) of stereotypical wild-type embryos from the early dermatogen up to the heart stage. (**E-H**) *brx* embryos with basal patterning defects at various stages (corresponding to A-D). (**I**) Penetrance of *brx* embryo phenotypes, scored from early dermatogen to heart stage. Uk-1, natural accession from which the *brx* loss-of-function allele was isolated; *brx*^{C}, introgression of the Uk-1 *brx* loss-of-function allele into the Col-0 background.

BRX is primarily a plasma membrane-associated protein

To corroborate our results in planta, we took advantage of transgenic *p35S::BRX:GFP* lines in which the BRX-GFP fusion protein could be observed by confocal microscopy in root tissue. Notably, BRX is a putative transcriptional regulator, which could localize to the nucleus in transiently transformed epidermal onion cells (Mouchel et al., 2004). Thus, we were surprised to observe BRX-GFP fluorescence localized nearly exclusively to the outline of cells in *Arabidopsis*, coinciding with the plasma membrane (Fig. 3C). Slight, patchy BRX-GFP in the cytosol was observed occasionally in less vacuolated, meristematic cells (Fig. 3D). Western blot analysis of cell fractionations (Bassham and Raikhel, 1998) detected BRX-GFP nearly exclusively in the microsomal fraction, similar to the integral membrane protein H^{+}-ATPase, but unlike an RNA polymerase subunit or GFP alone (Fig. 3F), thus biochemically verifying BRX membrane association. Finally, further verifying plasma membrane localization, BRX-GFP also

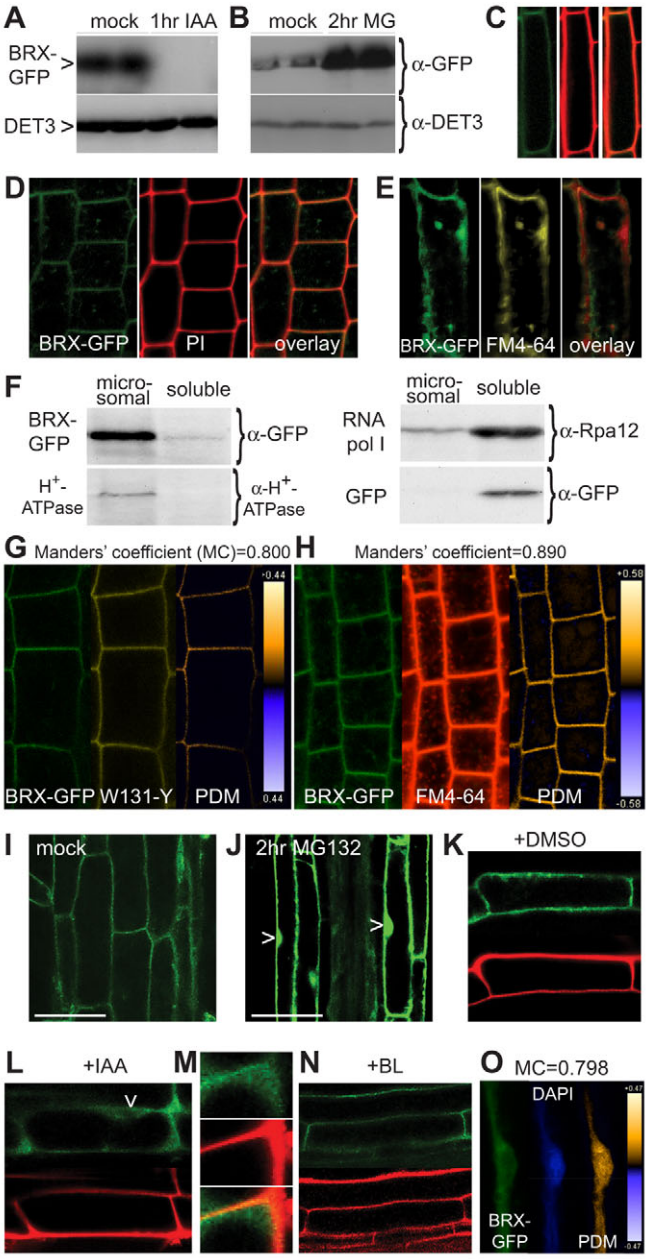

Fig. 3. Auxin-induced degradation and subcellular trafficking of BRX-GFP fusion protein. (**A**) Western blot analysis of transgenic *brx* seedlings complemented by expression of BRX-GFP fusion protein under control of the ubiquitous *35S* promoter (*p35S::BRX:GFP*). Seedlings were treated with solvent (mock) or 10 μM IAA for 1 hour. Endogenous DE-ETIOLATED 3 (DET3) protein served as a control. (**B**) Stabilization of BRX-GFP fusion protein in seedlings treated with 50 μM of the proteasome inhibitor MG132 (MG) for 2 hours. (**C**) Plasma membrane localization of BRX-GFP in *p35S::BRX:GFP* plants revealed by confocal microscopy (showing a cortex cell); left, BRX-GFP fluorescence; middle, propidium iodide (PI) cell wall staining; right, overlay. (**D**) As in C, showing multiple cortex cells in the root meristem. (**E**) BRX-GFP localization after 3 hours of 50 μM brefeldin A (BFA) treatment: left, BRX-GFP fluorescence; middle, staining of endosomal compartments by FM4-64 tracer dye; right, overlay. (**F**) Western blot analysis of microsomal and soluble protein fractions isolated from *p35S::BRX:GFP* (left and upper right) or *p35S::GFP* (lower right) seedlings, probed with antibodies against GFP, H^+-ATPase or the RNA polymerase I subunit RPA12. (**G**) Intensity correlation analysis (ICA) of BRX-GFP (left) and the citrine-based plasma membrane marker W131-Y (middle), and product of the differences from the mean (PDM) image (right, for the images to the left). Manders' coefficient: 0.0, no colocalization; 1.0, perfect colocalization. (**H**) ICA of BRX-GFP and FM4-64 dye in meristematic cells. (**I**) BRX-GFP fluorescence in root cells of *p35S::BRX:GFP* seedlings after 2 hours of mock treatment. (**J**) Stabilization of BRX-GFP and appearance in the nucleus (arrowheads) after 4 hours of 50 μM MG132 treatment. (**K-N**) *p35S::BRX:GFP* plants pretreated with 50 μM MG132 for 5 hours, then transferred into 30 μM cycloheximide and DMSO (mock, K), 10 μM IAA (L), or 10 pM brassinolide (BL, N) for 2 hours (BRX-GFP fluorescence versus PI staining). In the auxin treatment (L), BRX-GFP dissociates from the plasma membrane (M; top, BRX-GFP fluorescence; middle, PI staining; bottom, overlay) and persists in the nucleus (arrowhead). (**O**) ICA of BRX-GFP and DAPI staining of *p35S::BRX:GFP* plants treated with 50 μM MG132, 30 μM cycloheximide and 10 μM IAA for 90 minutes. Scale bars: 50 μm.

colocalized with the citrine-based plasma membrane marker W131-Y (Geldner et al., 2009) [Manders' overlap coefficient (MC)=0.800] (Manders et al., 1993) (Fig. 3G).

PINs are integral plasma membrane proteins that are continuously recycled to and from the membrane through the endocytic pathway (Geldner et al., 2003; Geldner et al., 2001). Treatment with the drug brefeldin A (BFA) disrupts this process and leads to the accumulation of PIN protein in endosomal, so-called BFA, compartments (Geldner et al., 2003). These can be identified by simultaneous labeling with the endocytic tracer dye FM4-64. Strikingly, after BFA application, BRX-GFP could also be found in BFA compartments (Fig. 3E). In the absence of BFA, FM4-64 progressively marks endosomes as it is taken up into the cell. Intensity correlation analysis (ICA) (Li et al., 2004) of FM4-64-labeled root cells with BRX-GFP signal could thus be used to verify endosomal BRX-GFP localization (MC=0.890; Fig. 3H). Together, our results suggest that BRX, similar to PIN proteins, is recycled through the endocytic pathway.

Auxin promotes translocation of BRX protein from the plasma membrane to the nucleus

Corroborating our western blot results in planta, BRX-GFP fluorescence increased upon MG132 treatment. Strikingly however, BRX-GFP fluorescence was now also observed in the nucleus (Fig. 3I,J). Thus, it appears that BRX can enter the nucleus, where it is turned over by proteasome-mediated degradation. To investigate in detail why BRX-GFP abundance decreases in response to auxin treatment, we circumvented the technically limiting factor of low BRX-GFP abundance by pretreating plants with MG132 before exposing them to auxin. At the same time as auxin treatment, we applied the protein biosynthesis inhibitor cycloheximide to exclude new BRX-GFP protein from entering the system. In both mock- and auxin-treated samples, nuclear BRX-GFP abundance gradually decreased as the effect of MG132 faded, consistent with the idea that BRX degradation is constitutive and that the biosynthesis of the factors involved does not depend on auxin. Moreover, it also became evident that auxin treatment promoted dissociation of BRX-GFP from the plasma membrane (Fig. 3L). This was accompanied by its occurrence in the cytoplasm (Fig. 3M) and extended persistence in the nucleus. Such behavior was never observed in controls, for instance in plants treated with solvent (mock; Fig. 3K) or brassinolide [which signals from the plasma membrane to the nucleus through the endocytic pathway (Geldner et al., 2007)] (Fig. 3N). Rather, in the controls BRX-GFP fluorescence swiftly disappeared from the nucleus after MG132 application was stopped,

but remained well visible at the plasma membrane. Finally, compared with controls, nuclear BRX-GFP accumulation was strongly accelerated by auxin treatment when MG132 was not administered prior to auxin and cycloheximide, but rather in parallel. ICA of respective DAPI-stained cells confirmed the notion that the nucleus was the target compartment (MC=0.798; Fig. 3O). Thus, the most parsimonious explanation for our observations is that plasma membrane-associated BRX protein translocates to the nucleus in response to auxin stimulus, eventually leading to BRX degradation.

BRX activity is required in the nucleus

The fact that BRX-GFP is hardly ever visible in the nucleus in the absence of proteasome inhibitor suggests that this degradation is an efficient constitutive process. To determine whether BRX entry into the nucleus is nevertheless required for its function, we assayed the subcellular localization of BRX fragments that displayed differential propensities to rescue the *brx* root growth phenotype. A GFP fusion protein with the conserved N-terminal domain of BRX (amino acids 1-57), excluding the conserved BRX domains, did not complement the mutant (Fig. 4C). This fusion protein was generally more abundant than full length BRX-GFP and was exclusively detected at the plasma membrane (Fig. 4A). By contrast, a GFP fusion protein comprising the BRX C-terminus (amino acids 139-344), including both BRX domains, significantly rescued *brx* root growth (Fig. 4C) and was not only detected at the plasma membrane, but also in the nucleus, even in the absence of MG132 (Fig. 4B). These results suggest that the N-terminus promotes BRX membrane association. Moreover, they suggest that efficient BRX degradation also requires N-terminal regions, as the C-terminal fusion protein was stabilized in the nucleus. In addition, the C-terminal fusion protein triggered a gain-of-function phenotype that was also occasionally observed in plants overexpressing full length BRX, i.e. a strongly elongated hypocotyl (Fig. 4D). Notably, a role for *BRX* in hypocotyl development has been described before (Sibout et al., 2008). Since the strength of this phenotype was either equal or higher in lines expressing the BRX C-terminus fusion protein as compared with full length BRX, this might also mean that the C-terminus is hyperactive and that the incomplete rescue of the short root phenotype could reflect auxin hypersensitivity (Li et al., 2009; Sibout et al., 2006). Most importantly however, collectively, our data suggest that the BRX C-terminus exerts an essential activity in the nucleus.

Consistent with the proposed role of *BRX* in transcriptional regulation, BRX can physically interact with a bona fide transcription factor of the B3 domain superfamily. This discovery originated from a yeast two hybrid screen, in which the BRX family protein, BRX-LIKE 4, was recovered as an interactor of NGATHA1 (NGA1) (Alvarez et al., 2006; Trigueros et al., 2009). Given the high level of conservation among BRX family genes (Briggs et al., 2006), it was not surprising that NGA1 could also interact with BRX (Fig. 4E). To verify this interaction in planta, we employed a bimolecular fluorescence complementation approach. Indeed, interaction of BRX and NGA1 was again observed, in the nuclei of transiently transformed tobacco leaf cells (Fig. 4F). Moreover, similar to *BRX*, *NGA1* is expressed in the root vasculature (Birnbaum et al., 2003; Trigueros et al., 2009). Thus, BRX might regulate transcription in conjunction with NGA1.

Interference of BRX activity with root gravitropism

The impact of auxin on BRX subcellular localization, together with the similarities between *BRX* and *PINs*, i.e. endocytic recycling and the penetrance and morphology of *brx* and multiple *pin* mutant

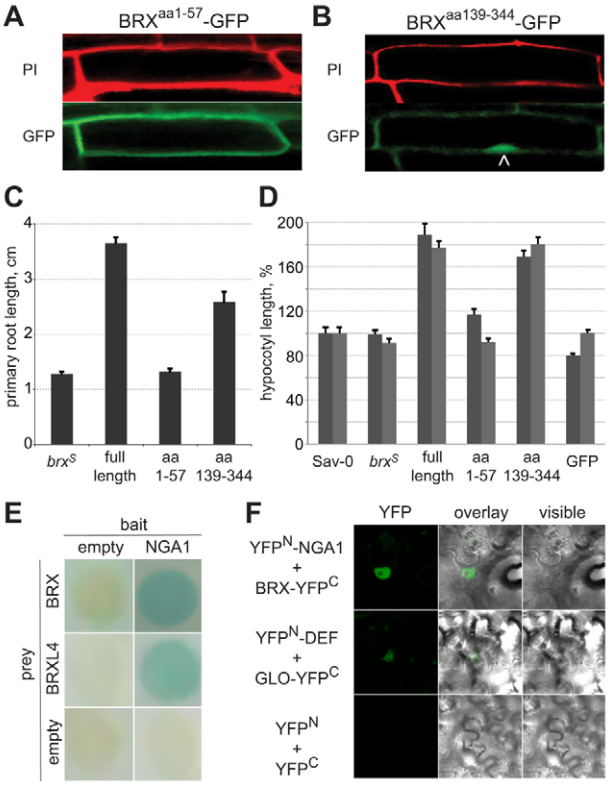

Fig. 4. Subcellular localization and gain-of-function effects of BRX fragments. (**A**) Bottom: subcellular localization of the BRX N-terminal fragment fusion protein (GFP fluorescence) at the plasma membrane. Top: PI staining. (**B**) Bottom: subcellular localization of the BRX C-terminal fragment fusion protein (GFP fluorescence) in the nucleus (arrowhead). Top: PI staining. (**C**) Propensity of fusion proteins between BRX fragments (amino acids indicated) and GFP to rescue the *brx* root growth defect. (**D**) Gain-of-function effects of BRX-GFP full length and fragment fusion proteins, and controls, on hypocotyl elongation (two replicate experiments). $n \geq 30$ seedlings in C and D. Error bars represent standard error of the mean. (**E**) Yeast two hybrid interactions between BRX family proteins and the NGA1 B3 domain transcription factor in the Matchmaker (Clontech) system. Positive interactions are indicated by colorimetric (blue color) colony assay. (**F**) Bimolecular fluorescence complementation in tobacco leaf cell nuclei between transiently expressed (*35S* promoter) full length NGA1 and BRX fusions to N- and C-terminal fragments of YFP, respectively. Known interaction between the MADS box transcription factors DEFICIENS (DEF) and GLOBOSA (GLO) served as a positive control. Right, visible; left, YFP fluorescence; middle, overlay.

embryo phenotypes (Blilou et al., 2005), prompted us to revisit whether *BRX* plays a direct role in PAT. Disrupting auxin transport does not only impinge on root growth, but also on tropic responses, such as gravitropism (Benjamins and Scheres, 2008; Leyser, 2005). This process is controlled by the columella root cap region, where dynamic relocalization of PIN proteins is required for proper gravitropism (Wisniewska et al., 2006). *BRX* is indeed expressed in the columella (Mouchel et al., 2006). However, *brx*, as well as *brx brxl1* double mutants, only displayed a very slight and background-dependent delay in gravitropism (see Fig. S1A,B in the supplementary material), which could also be an indirect consequence of its diminished root growth rate. If specifically targeted to the root cap however, excess BRX activity could delay root gravitropism (see Fig. S1B in the supplementary material). This

was also occasionally observed in strong *BRX* overexpression lines (see Fig. S1C in the supplementary material). Since root growth rate was restored in these lines, this suggests that the effect on tropism was genuine. Despite these gain-of-function phenotypes, and although *brx* root growth displays resistance to the auxin transport inhibitor naphthalene phthalamic acid (NPA) (Dhonukshe et al., 2008; Geldner et al., 2001; Petrasek et al., 2003), it appears unlikely that BRX is involved in the actual physical process of auxin transport (Mouchel et al., 2004; Mouchel et al., 2006). Corroborating this idea, we could not detect statistically significant differences in acropetal PAT in the roots of *brx* mutants when directly measured (E.S., three replicates, data not shown). Thus, in summary, although BRX is able to interfere with a PAT-related process, it does not appear to be an integral component of the auxin transport machinery.

Polar plasma membrane localization of BRX protein in vascular cells

A key feature of the inherent polarity of auxin transport is the asymmetric localization of the PAT machinery, in particular the PIN auxin efflux carriers (Wisniewska et al., 2006). For instance, PIN1 is typically located at the basal end (towards the root tip) of vascular root cells, in line with the direction of PAT. Similar asymmetric, polar localization of BRX-GFP at the basal end of vascular root cells, the expression domain of endogenous *BRX*, was evident in those transgenic *pBRX::BRX:GFP* individuals where fluorescence could be detected (Fig. 5A-C). No such signal was ever observed in extensive imaging of mutant and wild-type controls. Thus, in its genuine expression domain, BRX is asymmetrically located at the PIN1 auxin efflux carrier domain. Since expression of *BRX* under control of the *PIN1* promoter fully rescues the *brx* short root phenotype (Mouchel et al., 2006), the two genes do indeed appear to act in the same tissues.

BRX nuclear translocation might be a vesicle-based process

An important effect of auxin treatment is its effect on PIN protein abundance and distribution at the plasma membrane, which is likely to be mediated through auxin-induced changes in endosomal dynamics (Abas et al., 2006; Paciorek et al., 2005; Sauer et al., 2006). Thus, it appears possible that the auxin response of BRX-GFP reflects the effects of auxin on endocytosis. Indeed, slow-down of endocytic recycling by BFA treatment swiftly promoted BRX-GFP translocation to the nucleus (see Movie 1 in the supplementary material) and enhanced auxin effects on BRX-GFP. Notably, BFA specifically inhibits cargo delivery to membrane compartments from endosomal compartments (Geldner et al., 2003; Richter et al., 2007; Teh and Moore, 2007). Thus, disruption of endosomal BRX-GFP recycling to the plasma membrane could result in redirection of BRX-GFP transport towards the nucleus. This could also mean that BRX-GFP translocation to the nucleus might involve a vesicle-based step, a notion that is supported by the occurrence of trafficking BRX-GFP patches (see Movie 1 in the supplementary material).

Polar plasma membrane abundance of BRX protein responds to polar auxin transport inhibition

Since it has been suggested that auxin promotes its own efflux by stimulating PAT through its effect on endocytosis (Paciorek et al., 2005), the BRX-GFP response to auxin could reflect a response to increased PAT. To test this idea, we conducted the inverse experiment by taking advantage of the PAT inhibitor, NPA

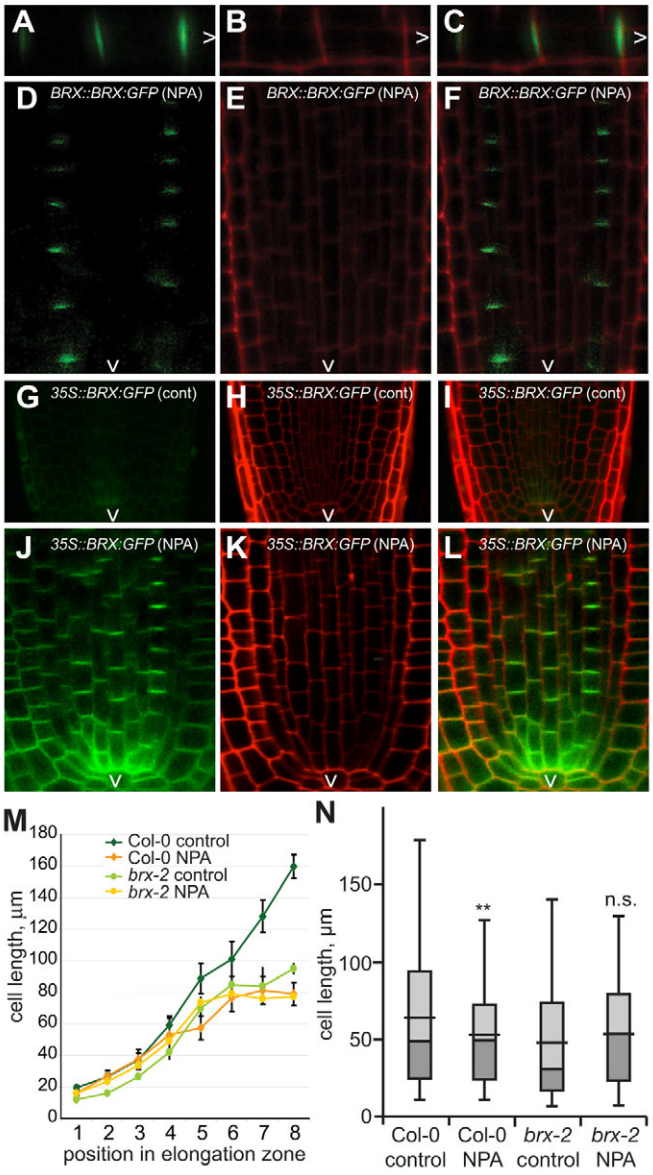

Fig. 5. Polar plasma membrane localization of BRX and response to auxin transport inhibition. (**A-C**) Polar plasma membrane localization of BRX-GFP expressed under its own promoter (*pBRX::BRX:GFP*) in root phloem pole cells: BRX-GFP fluorescence (A); corresponding PI staining (B); and overlay (C). (**D-F**) Stabilization of BRX-GFP fusion protein at its polar plasma membrane location in *pBRX::BRX:GFP* seedlings treated with 5 μM of the auxin transport inhibitor NPA for 10 hours. BRX-GFP fluorescence in the root phloem vasculature (images show the stele only), close to the root tip (D), corresponding PI staining (E) and overlay (F). (**G-L**) Stabilization and accumulation of BRX-GFP at its polar plasma membrane location after NPA treatment in *p35S::BRX:GFP* seedlings. (G-I) Mock treatment. (J-L) Similar to D-F, after 3 hours of NPA treatment. Images G-L were taken with identical intensity settings. (**M**) Average cell lengths in the root meristem elongation zone of 4-day-old seedlings, starting from the first rapidly elongating cell upwards, for wild type (Col-0) or *brx* mutants, after 16 hours of growth on control media or media containing 5 μM NPA. Sample size is 10-12 roots. Error bars represent standard error of the mean. (**N**) Size distribution of all cells measured in M, with average and quartiles indicated. Asterisks indicate *t*-test significance as compared with control treatment: $^{**}P<0.01$; n.s., not significant. *brx-2*: *brx* null allele in the Col-0 background. Arrowheads point towards the root tip.

(Dhonukshe et al., 2008; Geldner et al., 2001; Petrasek et al., 2003). Indeed, upon application of NPA at concentrations reported not to interfere with vesicle trafficking, BRX-GFP became stabilized at its polar plasma membrane localization in vascular cells. Thus, BRX-GFP became clearly visible in *pBRX::BRX:GFP* plants (Fig. 5D-F), in which it is hardly ever detectable under normal circumstances. This effect appeared to be non-genomic, as stabilization and polar accumulation of BRX-GFP could also be observed within less than 30 minutes of NPA treatment in plants in which *BRX:GFP* expression is no longer auxin-dependent (Fig. 5G-L). Thus, inhibition of PAT had an opposite effect on BRX-GFP localization as compared with auxin treatment. A plausible explanation for this observation would be that PAT inhibition also inhibited nuclear translocation of BRX-GFP, resulting in its increased plasma membrane abundance and stabilization.

PAT inhibition in wild type phenocopies the *brx* loss-of-function mutant

Notably, we had previously demonstrated that *brx* mutants are resistant to the inhibitory effects of NPA on root growth (Mouchel et al., 2006). In light of the above results, we revisited this physiological assay in more detail to determine the effect of NPA on a cellular level. We focused our investigation on the cell elongation zone of the root meristem, where *BRX* is genuinely expressed. Sixteen hours after transfer of 4-day-old wild-type or *brx* mutant seedlings from standard media to media containing 5 μM NPA, we compared the progression of cell elongation by measuring cell size, starting from the first rapidly elongating cell up to ten older neighboring cells in the same cell file. Whereas wild-type roots on control media displayed continuous elongation up to ~15 cells above the cell proliferation zone, cell elongation had already ceased at ~6 cells in the NPA-treated roots (Fig. 5M). Notably, the cell size profile of the NPA-treated wild-type roots closely matched the profile of control *brx* roots, which were again insensitive to NPA in this assay (Fig. 5M). Consistently, the overall cell size distribution of NPA-treated wild-type seedlings was significantly different from the mock-treated wild-type control, but not significantly different from the distribution in NPA- or mock-treated *brx* mutants (Fig. 5N). Thus, NPA treatment of wild-type roots phenocopied the root cell elongation phenotype of *brx* mutants.

DISCUSSION

In *Arabidopsis brx* mutants, root growth is strongly diminished and coincides with impaired auxin-responsive transcription (Mouchel et al., 2004; Mouchel et al., 2006). However, the latter could reflect an indirect effect of brassinosteroid deficiency, as both root growth and auxin-responsiveness of *brx* can be largely restored by brassinolide treatment (Mouchel et al., 2006). This interpretation is in line with a growing body of literature that suggests that brassinosteroids are rate-limiting for auxin action (Hardtke, 2007; Kuppusamy et al., 2008; Nemhauser et al., 2004; Vert et al., 2008). Our finding that the *hy5* mutation can significantly suppress the *brx* root growth phenotype supports this idea, as it suggests that a parallel constitutive increase in auxin-responsive transcription as conferred by *hy5* loss of function (Sibout et al., 2006) can offset diminished basic auxin-responsiveness of the transcriptional machinery in *brx*. This interpretation would also be consistent with more recent findings, which suggest that the brassinosteroid pathway modulates auxin-induced gene expression by lowering the level of constitutive repression, through impinging on the DNA-binding capacity of the repressive ARF2 (Vert et al., 2008). An indirect, brassinosteroid-mediated effect of BRX on ARF2 activity would also explain why auxin-responsiveness is impaired in *brx* mutants while at the same time canonical auxin signaling appears to remain intact.

An important feature of *BRX* is the control of its own expression by an autoregulatory feedback loop; *BRX* transcription is highly auxin-responsive and accordingly, *BRX* is no longer auxin-inducible and thus underexpressed in a *brx* background (Mouchel et al., 2006). Our results presented here suggest that auxin also controls BRX activity post-translationally, by negatively regulating the abundance of BRX protein. Since this could be counteracted by proteasome inhibitor treatment, BRX appears to be a target for auxin-induced, proteasome-mediated degradation. Interestingly, a salient feature of AUX/IAA corepressors is that their abundance is negatively regulated by auxin. Their respective genes, however, are themselves primary auxin-induced genes, which establishes a negative-feedback loop (Benjamins and Scheres, 2008; Dharmasiri et al., 2005a; Gray et al., 2001; Kepinski and Leyser, 2005). Thus, on both the transcriptional and post-translational level, BRX is controlled in a similar manner as AUX/IAAs. It therefore appears possible that BRX, just like AUX/IAAs, might be a substrate for TIR1-type auxin receptors. However, thus far, we could not detect any significant direct interaction between BRX and the prototypical auxin receptor, TIR1, using various approaches (K.S.O., unpublished). Therefore, BRX is possibly targeted for the proteasome pathway by other E3 ubiquitin ligases or, perhaps, BRX is stabilized by proteasome inhibitor treatment indirectly.

An alternative explanation for the negative regulation of BRX abundance by auxin is offered by the observed trafficking of BRX-GFP fusion protein from the plasma membrane to the nucleus. At steady state, BRX-GFP was nearly exclusively detectable at the plasma membrane. This is supported by our biochemical and colocalization studies. Since BRX contains neither secretion signals nor obvious modification sites for membrane anchor attachment, it appears that BRX is a membrane-associated protein. The plasma membrane localization of BRX-GFP together with its accumulation in BFA compartments after prolonged treatment, in the presence of cycloheximide, suggests that BRX is recycled through the endocytic pathway, similar to PIN proteins. Upon auxin treatment, BRX-GFP was released from the membrane and translocated to the nucleus. Interestingly, this effect could be mimicked by short BFA treatment, which also enhanced the effects of auxin if applied simultaneously. Notably, BFA specifically inhibits cargo delivery to membrane compartments by inactivating susceptible ARF-guanine nucleotide-exchange factors (ARF-GEFs). In *Arabidopsis* PAT, BFA specifically targets GNOM, an ARF-GEF that is involved in the plasma membrane delivery of PINs from endosomal compartments (Geldner et al., 2003; Richter et al., 2007; Teh and Moore, 2007). Thus, the BFA effect on BRX-GFP plasma membrane versus nuclear localization could be explained by a redirection of endosomal BRX-GFP transport towards the nucleus as redelivery to the plasma membrane becomes progressively blocked. This would also suggest that BRX-GFP translocation to the nucleus could, in part, be a vesicle-based process, a notion that is supported by the occurrence of trafficking BRX-GFP patches (see Movie 1 in the supplementary material). In summary, the most parsimonious explanation for our observations is that upon auxin stimulus, plasma membrane-associated BRX protein translocates to the nucleus, where it eventually is targeted for degradation by a constitutive, auxin-independent ubiquitin ligase.

It is noteworthy that, although our results are limited by the technical constraints on BRX-GFP detection, BRX-GFP abundance was considerably lower than GFP abundance in control lines using

the same constitutive promoter (typically <1/100) (Mouchel et al., 2006), consistent with high, efficient turnover of the protein. Thus, BRX-GFP was also less abundant than PIN1-GFP for instance, or BRI1-GFP expressed under control of their respective native promoters (Benkova et al., 2003; Geldner et al., 2007). These findings suggest that our experimental system was not overloaded by excess BRX-GFP.

Importantly, our analyses of BRX fragments suggest that despite its rapid turnover, BRX exerts an essential activity in the nucleus. Based on our protein interaction studies and overlapping expression domains (Birnbaum et al., 2003; Trigueros et al., 2009), this activity probably involves the B3 domain transcription factor NGA1. BRX might regulate the transcription of genes controlled by NGA1 by acting as a transcriptional coregulator, since so far we could not detect DNA-binding activity of BRX (C.S.H., unpublished). Although the exact role of NGA1 in root development remains to be explored, it is interesting to note that NGA1 is a B3 domain transcription factor that is related to ARFs. Thus, one possibility is that BRX family proteins and NGA family transcription factors could form novel coregulator-transcription factor pairs, whose regulatory logic is conceptually similar to the AUX/IAA-ARF transcriptional switches, and whose activity is also controlled by auxin.

This control is possibly exerted through auxin flux, as NPA treatment resulted in stabilization of BRX-GFP and its increased abundance at the polar PIN1 auxin efflux carrier domain. An alternative explanation for this accumulation at the plasma membrane could be increased cellular auxin concentration, due to inhibition of auxin efflux (and thus increased *BRX* transcription). However, this would be difficult to reconcile with the opposite effect of auxin treatment on BRX-GFP localization. Moreover, the effect of NPA treatment appeared to be non-genomic: stabilization and polar accumulation of BRX-GFP could also be observed in plants in which *BRX:GFP* expression is no longer auxin-dependent. A plausible explanation for this observation would be that PAT inhibition prevented nuclear translocation of BRX-GFP. This interpretation would also explain the morphological effects of NPA treatment on the root meristem, in the sense that in the context of root cell elongation, NPA treatment might largely act through promoting BRX plasma membrane association, thus abolishing BRX activity in the nucleus and consequently mimicking the *brx* loss-of-function phenotype.

Conclusions

In summary, we provide evidence that BRX is a plasma membrane-associated protein, which can translocate into the nucleus to regulate gene expression. Moreover, BRX appears to be localized at the PIN1 auxin efflux carrier domain and the extent of this plasma membrane localization versus transfer to the nucleus appears to respond to auxin activity, and possibly to the rate of polar auxin transport. Collectively, our results suggest that BRX is involved in a novel intracellular signaling pathway, which might act to convey auxin action at the efflux carrier domain into gene expression differences. Since *brx* mutants are impaired in cell proliferation and elongation, but not in lateral organ formation or tropisms, this facet of auxin signaling could mainly serve to control cellular growth. Conceptually, this pathway could thus serve as an important contextual readout of the auxin gradient observed across the root tip.

The authors thank Prof. N. Geldner for helpful comments on the manuscript and for the W131-Y plasma membrane marker line; Dr Rodriguez-Egea for the *brx-2* allele; Dr Brendan Davies and Barry Causier for help with yeast two hybrid experiments; Dr Alejandro Ferrando for providing BiFC plasmids; and Profs C. Fankhauser and K. Schumacher for anti-DET3 antibody. Work in the lab of C.F. was supported by grant BIO2005-01541 from the Ministerio de Educación y Ciencia of Spain, and by doctoral fellowships of the Generalitat Valenciana to M.N.-G. and M.T. Work in the lab of C.S.H. was supported by Swiss National Science Foundation grant 3100A0-107631, 'BRAVISSIMO' Marie-Curie Initial Training Network support for E.S., a Marie-Curie post-doctoral fellowship to K.S.O. and University of Lausanne support for J.B. We would also like to acknowledge support of the Cellular Imaging Facility of the University of Lausanne.

Author contributions

C.S.H., E.S. and K.S.O. conceived this study and wrote the manuscript with help from J.B., P.S. and C.F.; E.S. provided the data for Fig. 2, Fig. 3C-E,G-O, Fig. 4A,B,D, Fig. 5 and Movie 1; K.S.O. provided the data for Fig. 1H-K, Fig. 3A,B and Fig. 4C, and the materials for Fig. 4; J.B. provided the data for Fig. S1 and the materials for Fig. 1D-G; P.S. provided the data for Fig. 3F; M.T. provided the data for Fig. 4E; M.N.-G. provided the data for Fig. 4F; C.S.H. provided the data for Fig. 1A-G.

Supplementary material

Supplementary material for this article is available at http://dev.biologists.org/cgi/content/full/136/12/2059/DC1

References

Abas, L., Benjamins, R., Malenica, N., Paciorek, T., Wisniewska, J., Moulinier-Anzola, J. C., Sieberer, T., Friml, J. and Luschnig, C. (2006). Intracellular trafficking and proteolysis of the Arabidopsis auxin-efflux facilitator PIN2 are involved in root gravitropism. *Nat. Cell Biol.* **8**, 249-256.

Alvarez, J. P., Pekker, I., Goldshmidt, A., Blum, E., Amsellem, Z. and Eshed, Y. (2006). Endogenous and synthetic microRNAs stimulate simultaneous, efficient, and localized regulation of multiple targets in diverse species. *Plant Cell* **18**, 1134-1151.

Badescu, G. O. and Napier, R. M. (2006). Receptors for auxin: will it all end in TIRs? *Trends Plant Sci.* **11**, 217-223.

Bassham, D. C. and Raikhel, N. V. (1998). An Arabidopsis VPS45p homolog implicated in protein transport to the vacuole. *Plant Physiol.* **117**, 407-415.

Bauby, H., Divol, F., Truernit, E., Grandjean, O. and Palauqui, J. C. (2007). Protophloem differentiation in early Arabidopsis thaliana development. *Plant Cell Physiol.* **48**, 97-109.

Benjamins, R. and Scheres, B. (2008). Auxin: the looping star in plant development. *Annu. Rev. Plant Biol.* **59**, 443-465.

Benkova, E., Michniewicz, M., Sauer, M., Teichmann, T., Seifertova, D., Jurgens, G. and Friml, J. (2003). Local, efflux-dependent auxin gradients as a common module for plant organ formation. *Cell* **115**, 591-602.

Birnbaum, K., Shasha, D. E., Wang, J. Y., Jung, J. W., Lambert, G. M., Galbraith, D. W. and Benfey, P. N. (2003). A gene expression map of the Arabidopsis root. *Science* **302**, 1956-1960.

Blilou, I., Xu, J., Wildwater, M., Willemsen, V., Paponov, I., Friml, J., Heidstra, R., Aida, M., Palme, K. and Scheres, B. (2005). The PIN auxin efflux facilitator network controls growth and patterning in Arabidopsis roots. *Nature* **433**, 39-44.

Briggs, G. C., Mouchel, C. F. and Hardtke, C. S. (2006). Characterization of the plant-specific BRX gene family reveals limited genetic redundancy despite high sequence conservation. *Plant Physiol.* **140**, 1306-1316.

Curtis, M. D. and Grossniklaus, U. (2003). A gateway cloning vector set for high-throughput functional analysis of genes in planta. *Plant Physiol.* **133**, 462-469.

Dharmasiri, N., Dharmasiri, S. and Estelle, M. (2005a). The F-box protein TIR1 is an auxin receptor. *Nature* **435**, 441-445.

Dharmasiri, N., Dharmasiri, S., Weijers, D., Lechner, E., Yamada, M., Hobbie, L., Ehrismann, J. S., Jurgens, G. and Estelle, M. (2005b). Plant development is regulated by a family of auxin receptor F box proteins. *Dev. Cell* **9**, 109-119.

Dhonukshe, P., Grigoriev, I., Fischer, R., Tominaga, M., Robinson, D. G., Hasek, J., Paciorek, T., Petrasek, J., Seifertova, D., Tejos, R. et al. (2008). Auxin transport inhibitors impair vesicle motility and actin cytoskeleton dynamics in diverse eukaryotes. *Proc. Natl. Acad. Sci. USA* **105**, 4489-4494.

Friml, J., Vieten, A., Sauer, M., Weijers, D., Schwarz, H., Hamann, T., Offringa, R. and Jurgens, G. (2003). Efflux-dependent auxin gradients establish the apical-basal axis of Arabidopsis. *Nature* **426**, 147-153.

Geldner, N., Friml, J., Stierhof, Y. D., Jurgens, G. and Palme, K. (2001). Auxin transport inhibitors block PIN1 cycling and vesicle trafficking. *Nature* **413**, 425-428.

Geldner, N., Anders, N., Wolters, H., Keicher, J., Kornberger, W., Muller, P., Delbarre, A., Ueda, T., Nakano, A. and Jurgens, G. (2003). The Arabidopsis GNOM ARF-GEF mediates endosomal recycling, auxin transport, and auxin-dependent plant growth. *Cell* **112**, 219-230.

Geldner, N., Hyman, D. L., Wang, X., Schumacher, K. and Chory, J. (2007). Endosomal signaling of plant steroid receptor kinase BRI1. *Genes Dev.* **21**, 1598-1602.
Geldner, N., Dénervaud-Tendon, V., Hyman, D. L., Mayer, U., Stierhof, Y. D. and Chory, J. (2009). Rapid, combinatorial analysis of membrane compartments in intact plants with a multi-color marker set. *Plant J.* doi: 10.1111/j.1365-313X.2009.03851.x
Gray, W. M., Kepinski, S., Rouse, D., Leyser, O. and Estelle, M. (2001). Auxin regulates SCF(TIR1)-dependent degradation of AUX/IAA proteins. *Nature* **414**, 271-276.
Grieneisen, V. A., Xu, J., Maree, A. F., Hogeweg, P. and Scheres, B. (2007). Auxin transport is sufficient to generate a maximum and gradient guiding root growth. *Nature* **449**, 1008-1013.
Hamann, T., Benkova, E., Baurle, I., Kientz, M. and Jurgens, G. (2002). The Arabidopsis BODENLOS gene encodes an auxin response protein inhibiting MONOPTEROS-mediated embryo patterning. *Genes Dev.* **16**, 1610-1615.
Hardtke, C. S. (2007). Transcriptional auxin-brassinosteroid crosstalk: who's talking? *BioEssays* **29**, 1115-1123.
Hardtke, C. S. and Berleth, T. (1998). The Arabidopsis gene MONOPTEROS encodes a transcription factor mediating embryo axis formation and vascular development. *EMBO J.* **17**, 1405-1411.
Hardtke, C. S., Ckurshumova, W., Vidaurre, D. P., Singh, S. A., Stamatiou, G., Tiwari, S. B., Hagen, G., Guilfoyle, T. J. and Berleth, T. (2004). Overlapping and non-redundant functions of the Arabidopsis auxin response factors MONOPTEROS and NONPHOTOTROPIC HYPOCOTYL 4. *Development* **131**, 1089-1100.
Kepinski, S. and Leyser, O. (2005). The Arabidopsis F-box protein TIR1 is an auxin receptor. *Nature* **435**, 446-451.
Kuppusamy, K. T., Walcher, C. L. and Nemhauser, J. L. (2008). Cross-regulatory mechanisms in hormone signaling. *Plant Mol. Biol*. **69**, 375-381.
Leyser, O. (2005). Auxin distribution and plant pattern formation: how many angels can dance on the point of PIN? *Cell* **121**, 819-822.
Li, H., Cheng, Y., Murphy, A., Hagen, G. and Guilfoyle, T. J. (2009). Constitutive repression and activation of auxin signaling in Arabidopsis. *Plant Physiol*. **149**, 1277-1288.
Li, Q., Lau, A., Morris, T. J., Guo, L., Fordyce, C. B. and Stanley, E. F. (2004). A syntaxin 1, G alpha(o), and N-type calcium channel complex at a presynaptic nerve terminal: Analysis by quantitative immunocolocalization. *J. Neurosci.* **24**, 4070-4081.
Manders, E. M. M., Verbeek, F. J. and Aten, J. A. (1993). Measurement of colocalization of objects in dual-color confocal images. *J. Microsc.* **169**, 375-382.
Men, S., Boutte, Y., Ikeda, Y., Li, X., Palme, K., Stierhof, Y. D., Hartmann, M. A., Moritz, T. and Grebe, M. (2008). Sterol-dependent endocytosis mediates post-cytokinetic acquisition of PIN2 auxin efflux carrier polarity. *Nat. Cell Biol.* **10**, 237-244.
Mouchel, C. F., Briggs, G. C. and Hardtke, C. S. (2004). Natural genetic variation in Arabidopsis identifies BREVIS RADIX, a novel regulator of cell proliferation and elongation in the root. *Genes Dev.* **18**, 700-714.
Mouchel, C. F., Osmont, K. S. and Hardtke, C. S. (2006). BRX mediates feedback between brassinosteroid levels and auxin signalling in root growth. *Nature* **443**, 458-461.
Nemhauser, J. L., Mockler, T. C. and Chory, J. (2004). Interdependency of brassinosteroid and auxin signaling in Arabidopsis. *PLoS Biol.* **2**, E258.
Paciorek, T., Zazimalova, E., Ruthardt, N., Petrasek, J., Stierhof, Y. D., Kleine-Vehn, J., Morris, D. A., Emans, N., Jurgens, G., Geldner, N. et al. (2005). Auxin inhibits endocytosis and promotes its own efflux from cells. *Nature* **435**, 1251-1256.
Petrasek, J., Cerna, A., Schwarzerova, K., Elckner, M., Morris, D. A. and Zazimalova, E. (2003). Do phytotropins inhibit auxin efflux by impairing vesicle traffic? *Plant Physiol.* **131**, 254-263.
Reinhardt, D., Mandel, T. and Kuhlemeier, C. (2000). Auxin regulates the initiation and radial position of plant lateral organs. *Plant Cell* **12**, 507-518.
Richter, S., Geldner, N., Schrader, J., Wolters, H., Stierhof, Y. D., Rios, G., Koncz, C., Robinson, D. G. and Jurgens, G. (2007). Functional diversification of closely related ARF-GEFs in protein secretion and recycling. *Nature* **448**, 488-492.
Sabatini, S., Beis, D., Wolkenfelt, H., Murfett, J., Guilfoyle, T., Malamy, J., Benfey, P., Leyser, O., Bechtold, N., Weisbeek, P. et al. (1999). An auxin-dependent distal organizer of pattern and polarity in the Arabidopsis root. *Cell* **99**, 463-472.
Sauer, M., Balla, J., Luschnig, C., Wisniewska, J., Reinohl, V., Friml, J. and Benkova, E. (2006). Canalization of auxin flow by Aux/IAA-ARF-dependent feedback regulation of PIN polarity. *Genes Dev.* **20**, 2902-2911.
Sibout, R., Sukumar, P., Hettiarachchi, C., Holm, M., Muday, G. K. and Hardtke, C. S. (2006). Opposite root growth phenotypes of hy5 versus hy5 hyh mutants correlate with increased constitutive auxin signaling. *PLoS Genet.* **2**, e202.
Sibout, R., Plantegenet, S. and Hardtke, C. S. (2008). Flowering as a condition for xylem expansion in Arabidopsis hypocotyl and root. *Curr. Biol.* **18**, 458-463.
Strader, L. C., Monroe-Augustus, M. and Bartel, B. (2008). The IBR5 phosphatase promotes Arabidopsis auxin responses through a novel mechanism distinct from TIR1-mediated repressor degradation. *BMC Plant Biol.* **8**, 41.
Teh, O. K. and Moore, I. (2007). An ARF-GEF acting at the Golgi and in selective endocytosis in polarized plant cells. *Nature* **448**, 493-496.
Tiwari, S. B., Hagen, G. and Guilfoyle, T. J. (2004). Aux/IAA proteins contain a potent transcriptional repression domain. *Plant Cell* **16**, 533-543.
Trigueros, M., Navarrete-Gómez, M., Sato, S., Christensen, S., Pelaz, S., Weigel, D., Yanofsky, M. and Ferrándiz, C. (2009). The NGATHA genes direct style development in the Arabidopsis gynoecium. *Plant Cell* (in press).
Ulmasov, T., Hagen, G. and Guilfoyle, T. J. (1997). ARF1, a transcription factor that binds to auxin response elements. *Science* **276**, 1865-1868.
Vert, G., Walcher, C. L., Chory, J. and Nemhauser, J. L. (2008). Integration of auxin and brassinosteroid pathways by Auxin Response Factor 2. *Proc. Natl. Acad. Sci. USA* **105**, 9829-9834.
Vieten, A., Vanneste, S., Wisniewska, J., Benkova, E., Benjamins, R., Beeckman, T., Luschnig, C. and Friml, J. (2005). Functional redundancy of PIN proteins is accompanied by auxin-dependent cross-regulation of PIN expression. *Development* **132**, 4521-4531.
Voinnet, O., Rivas, S., Mestre, P. and Baulcombe, D. (2003). An enhanced transient expression system in plants based on suppression of gene silencing by the p19 protein of tomato bushy stunt virus. *Plant J.* **33**, 949-956.
Wisniewska, J., Xu, J., Seifertova, D., Brewer, P. B., Ruzicka, K., Blilou, I., Rouquie, D., Benkova, E., Scheres, B. and Friml, J. (2006). Polar PIN localization directs auxin flow in plants. *Science* **312**, 883.